

AAEC/E502



JOHN
TRN AUG10 6210

AAEC/E502

AUSTRALIAN ATOMIC ENERGY COMMISSION
RESEARCH ESTABLISHMENT
LUCAS HEIGHTS

DEEP LEVEL TRANSIENT SPECTROSCOPY OF γ -RAY
INDUCED DEFECTS IN GERMANIUM

by

S.J. PEARTON
A.A. WILLIAMS
A.J. TAVENDALE

December 1980

ISBN 0 642 59699 9

AUSTRALIAN ATOMIC ENERGY COMMISSION
RESEARCH ESTABLISHMENT
LUCAS HEIGHTS

DEEP LEVEL TRANSIENT SPECTROSCOPY
OF γ -RAY INDUCED DEFECTS IN GERMANIUM

by

S.J. PEARTON*
A.A. WILLIAMS
A.J. TAVENDALE

ABSTRACT

Deep level transient capacitance spectroscopy has been used to examine γ -ray induced defect centres in germanium crystals grown at the AAEC Research Establishment under widely varying conditions. A deep acceptor level at $E_V + 0.38$ eV has been observed for the first time in all p-type samples; this was removed by annealing at 675°C for three hours. A new, deep donor level at $E_C - 0.42$ eV observed in n-type material was not removed by this procedure.

* AINSE postgraduate Student on attachment to the AAEC from Physics Department, University of Tasmania

National Library of Australia card number and ISBN 0 642 59699 9

The following descriptors have been selected from the INIS Thesaurus to describe the subject content of this report for information retrieval purposes. For further details please refer to IAEA-INIS-12 (INIS: Manual for Indexing) and IAEA-INIS-13 (INIS: Thesaurus) published in Vienna by the International Atomic Energy Agency.

GERMANIUM; PHYSICAL RADIATION EFFECTS; GE SEMICONDUCTOR DETECTORS;
GAMMA RADIATION; CRYSTALS; IRRADIATION; SPECTROSCOPY; INTERSTITIALS;
VACANCIES

CONTENTS

1. INTRODUCTION	1
2. EXPERIMENTAL DETAILS	1
3. MEASUREMENTS	2
4. DISCUSSION	3
5. SUMMARY	5
6. ACKNOWLEDGEMENTS	5
7. REFERENCES	5
Table 1 Material Pre-irradiation	7
Table 2 Material Post-irradiation	9
Figure 1 Deep level transient spectrum of 78-93-4 post-irradiation	11
Figure 2 Deep level transient spectrum of 78-93-6 post-irradiation	11
Figure 3 Deep level transient spectrum of 78-48-4 post-irradiation	12
Figure 4 Deep level transient spectrum of 78-8-6 (H ₂ -rich) post-irradiation	12
Figure 5 Deep level transient spectrum of 77-93-4 post-irradiation	13
Figure 6 Deep level transient spectrum of 78-8-6 (H ₂ -poor) pre-irradiation	13
Figure 7 Arrhenius plots for some defect levels observed in germanium	14
Figure 8 Relative signal output v. pulse width for some defect levels in germanium	15
Figure 9 Relative capacitance change v. pulse amplitude for some defect levels in germanium	15

1. INTRODUCTION

The effect of radiation damage on germanium nuclear radiation detectors is important to their performance. Ionising radiation introduces defect centres which act as trapping and recombination centres to the charge released by an incoming particle or photon. The consequent lowering of charge collection efficiency leads to poorer energy resolution, characterised by 'tailing' on the low energy side of spectrum peaks, until at large integrated fluxes ($> 10^9 \text{ cm}^{-2}$ for protons and α -particles) the detector is no longer usable. In many cases, the detector may be returned to virtually its original state by thermal annealing at temperatures in excess of 400°C , which removes the radiation-induced defect levels [Mayer 1968].

The technique of Deep Level Transient Spectroscopy (DLTS), introduced by Lang [1974], is ideal for the study of radiation damage in semiconductors. It has the advantage of allowing individual defect levels to be monitored as a function of radiation dose or annealing time.

This report presents results on defect levels introduced by gamma-irradiation of germanium of both conductance types grown under a wide range of conditions at the AAEC Research Establishment and demonstrates that, in some cases, impurity-defect centres are introduced that cannot be removed by thermal annealing at 675°C . The high sensitivity of the DLTS technique has revealed a large number of γ -ray induced levels. The extremely low density of many levels makes positive identification impossible at present.

2. EXPERIMENTAL DETAILS

Eight diodes were prepared from material grown at the Research Establishment. Details of the crystals are given in Table 1. Samples were cut from the parent crystals and lapped into the shape of a disc or cube. Net electrically-active impurity densities were determined from measurements of the diode capacitances at a standard temperature (77 K).

For both n- and p-type materials, a similar preparation was followed. After polishing with a slurry of 600 grade SiC grit on pile cloth, the samples were etched in a 4:1 mixture of HNO_3 (70 wt %) and HF (40 wt %). Lithium diffusion (10 minutes at 325°C) by evaporation from a metallic Li source was used for the n^+ contact, and evaporation of a thin palladium metal film

provided a barrier contact. Samples of p-type conductance depleted from the n^+ contact, whereas n-type samples depleted from the Pd barrier.

An Oxford Instruments continuous flow cryostat was used to cycle samples from 5 K to 300 K. The cryostat and DLTS system have been described elsewhere [Pearson et al. 1980].

For annealing experiments both contacts were lapped off and replaced after the heat treatment. The samples were covered in GaIn alloy to prevent indiffusion of impurities, and the annealing performed under H_2 .

The samples were scanned for trapping centres before irradiation so that defects induced by the radiation could be identified. Briefly, the Schottky barrier or p-n junction under test is reverse biased and majority traps are filled by zero bias pulsing, resulting in a collapse of the depletion region. Minority carriers may be introduced by an infrared light emitting diode for Schottky barriers, or by forward bias pulsing for p-n junctions. As the sample is cycled in temperature, thermal emission of trapped carriers results in exponential capacitance transients detected by a Boonton 71A capacitance bridge. When the thermal emission rate from a particular trap matches that produced by an electronic correlator having an exponential function reference generator [Miller et al. 1975], a peak occurs in the correlator output. A trap spectrum is produced by employing an X-Y recorder to plot correlator output versus temperature.

3. MEASUREMENTS

Table 1 lists the materials and results obtained before the irradiation. Defects were labelled by the temperatures at which they appeared for a correlator time constant of 10 ms. The energy separation of the defect from the appropriate band edge was obtained by measuring the thermal emission rate as a function of temperature. Capture cross sections were measured by following the capacitance signal output as a function of the pulse duration. Cross sections can also be derived from a graph of the intercept of the emission rate versus temperature. Variability in the two measurements was expected since one was for the neutral material whereas the other occurred in the depleted material. Trap concentrations were obtained by measuring the relative change in correlator output produced by a small change in the pulse amplitude. Defect densities can also be profiled by taking advantage of the

change of depletion depth of a p-n junction in a Schottky barrier device with applied bias.

Table 2 shows the measured defect levels after the diodes had been irradiated with Co-60 γ -rays to a dose of 1500 kGy (150 Mrad), sufficient to produce a significant number of trapping centres. As with the unirradiated material, energy levels were corrected for the temperature dependence of the emission rate by subtracting $2kT$ from the raw energy obtained, where T is the average temperature of the peak position over the set of time constants used [Miller, Lang and Kimerling 1977]. Estimated energies were obtained from the equation

$$e_n = \frac{\sigma_n \langle v_n \rangle N_c}{g} \exp\left(\frac{-\Delta E}{kT}\right) \quad (1)$$

where e_n = emission rate of electrons from trapping centre, σ_n = capture cross section of trap for electrons, $\langle v_n \rangle$ = average thermal velocity of free carrier, N_c = density of states in the conduction band, ΔE = energy separation of level from conduction band, k = Boltzmann's constant, and T = absolute temperature at which peak occurs. A typical value of $\sigma = 10^{-14} \text{ cm}^2$ was assumed for the estimated energies. In such cases, the most probable errors are ± 10 per cent, whereas for others they are ± 7 per cent. Typical errors for the cross sections are ± 30 per cent, and for the concentrations ± 25 per cent. The free carrier densities used to determine defect concentrations were measured at the peak temperatures averaged over up and down temperature scans.

Figures 1-5 show typical DLT spectra from irradiated germanium samples of both conductance types and Figure 6 shows a spectrum from an unirradiated sample. Figure 7 displays the Arrhenius plots of some of the major defect levels observed in the material and Figure 8 the data used to obtain capture cross sections. Defects caused by a γ -ray flux uniformly irradiating the whole sample would be expected to have a constant profile, and this is shown to be the case for common levels introduced (Figure 9).

4. DISCUSSION

A comparison of Tables 1 and 2 shows the tendency for n-type material to compensate (i.e. achieve balance of donors and acceptors) upon irradiation, whereas in p-type the introduction of radiation-induced acceptor levels causes an increase in free carrier density. A significant feature is the

introduction of a very deep acceptor, $E_V + 0.38$ eV, into the three p-type samples and a very deep donor, $E_C - 0.42$ eV, into four out of five n-type samples. The $E_V + 0.38$ eV level was removed after annealing at 675°C for 3 hours, as was expected of a primary radiation defect; however, the $E_C - 0.42$ eV level remained after the heat treatment. A similar behaviour has been observed in a deep donor level ($E_C - 0.36$ eV) introduced by long-term annealing of n-type Ge at room temperature [Pearton et al. 1980]. The stability of the $E_C - 0.42$ eV defect suggests the formation of a stable electrically-active complex, e.g. oxide, possibly involving silicon and/or phosphorus, two impurities known to be present in this type of germanium. Another possibility is a complex such as P-Si-V; however, only speculation on its structure is possible at this stage.

The level introduced at $E_V + 0.23$ eV in two of the p-type samples appears to be related to H_2 , because it is absent from the H_2 -poor material. This level has also been produced in an n-type sample grown under dry N_2 gas. The effect of H_2 in complexing levels is seen when comparing results from the H_2 -rich and H_2 -poor samples. The $E_V + 0.21$ eV level induced in diodes 77-85-4 and 78-8-6, which has been seen previously in e-irradiated material [Laurence and Albany 1971], was present originally in the H_2 -poor material. The $E_V + 0.36$ eV acceptor level seen previously in irradiated material [Curtis and Crawford 1961; Akimchenko et al. 1963; Srouf and Curtis 1971; Basman et al. 1974] is also present in some of the unirradiated samples. The $E_V + 0.33$ eV level observed in 78-8-6 H_2 -poor has been assigned to copper [Haller et al. 1977], and has been seen as a recombination centre in As- and Sb-doped material [Srouf and Curtis 1971; Laurence and Albany 1971]. The acceptor $E_V + 68$ meV in 78-93-4 is either the well known divacancy-hydrogen level [Evwaraye et al. 1979; Haller et al. 1979] or oxygen [Haller et al. 1979]. The $E_V + 0.10 - 0.16$ eV levels, which are common in e- and γ -irradiated n-type materials, are assigned to group V donor-radiation induced acceptor complexes [Mashovets 1977].

Of particular interest is the diode 78-93-4, high purity p-type material.

Such material is used for making high resolution nuclear radiation detectors which, although operated at 77 K, are able to be stored at room temperature, in contrast to the familiar Ge(Li) detectors which must be constantly maintained at liquid N_2 temperature. It is most likely that this particular sample would prove mediocre as a spectrometer. Both electron and hole traps are present at 77 K ($\sim 10^{-2}$ of the background doping density), the effect of the electron traps extending from 20 - 110 K, and the hole (majority) traps

from 5 - 160 K. It is known that trapping and retention of 10^{-4} of the charge released by an ionising particle leads to tailing on energy spectra [Haller et al. 1979]. In this case, tailing was observed on the low energy side of spectra produced by detectors from this material. This illustrates that DLTS may be used to confirm charge trapping as a reason for poor energy resolution in a detector. Samples used on DLTS must initially be in the form of a radiation detector, so no additional preparation is required for the sample to be used as a detector or DLTS sample.

5. SUMMARY

New deep donor and acceptor levels have been observed in γ -irradiated Ge by DLTS. The deepest of the acceptors, $E_V + 0.38$ eV, was removed by annealing at 675°C. The deepest of the donors, $E_C - 0.42$ eV, was stable at this temperature. It is suspected that the latter level is caused by the formation of a stable oxide or other such impurity complex. The capacitance transient technique, applied here for the first time to γ -radiation defects in Ge, has proved ideal for their study.

6. ACKNOWLEDGEMENTS

The authors wish to thank Mr G.C. Wall who kindly supplied much of the material and Dr E.M. Lawson for his support and encouragement. The technical assistance of Mr D. Alexiev in annealing the samples and wiring the correlator, and Mr A. McG. Beech in sample preparation and instrumentation, is appreciated. One of us (SJP) acknowledges the support of an Australian Institute of Nuclear Science and Engineering (AINSE) postgraduate scholarship.

7. REFERENCES

- Akimchenko, I.P., Vavilov, V.A. and Plotnikov, A.F. [1963] - Fiz. Tverd. Tela, 5:1417; Sov. Phys. - Solid. State, 5:1031.
- Basman, A.R., Gerasimov, A.B., Kakhidze, N.G., Konovalenko, B.M. and Tsertsvadze, A.A. [1974] - Sov. Phys. - Semicond., 7(7)903.

- Curtis, O.L. and Crawford, J.H. Jr. [1961] - Phys. Rev., 124:731.
- Ewaraye, A.O., Hall, R.N. and Soltys, T.J. [1979] - IEEE Trans. Nucl. Sci., 26(1)279.
- Haller, E.E., Hubbard, G.S. and Hansen, W.L. [1977] - IEEE Trans. Nucl. Sci., 24(1)48.
- Haller, E.E., Li, P.P., Hubbard, G.S. and Hansen, W.L. [1979] - IEEE Trans. Nucl. Sci., 26(1)265.
- Lang, D.V. [1974] - J. Appl. Phys., 45:3023.
- Laurence, G. and Albany, H.J. [1971] - Radiation Effects in Semiconductors (eds. J.W. Corbett and G.D. Watkins), Gordon and Breach, London, p.113.
- Mashovets, T.V. [1977] - Radiation Effects in Semiconductors, Inst. Physics Conf., Series No.31, p.30.
- Mayer, J.W. [1968] - Semiconductor Detectors (eds. G. Bertolini and A. Coche), North Holland, Amsterdam, p.445
- Miller, G.L., Ramirez, J.V. and Robertson, D.A.H. [1975] - J. Appl. Phys., 46(6)2638.
- Miller, G.L., Lang, D.V. and Kimerling, L.C. [1977] - Ann. Rev. Mater. Sci., pp. 377-448.
- Pearton, S.J., Williams, A.A., Tavendale, A.J. and Lawson, E.M. [1980] - AAEC/E501.
- Srour, J.R. and Curtis, O.L. Jr. [1971] - Radiation Effects in Semiconductors (eds. J.W. Corbett and G.D. Watkins), Gordon and Breach, London, p.113.

TABLE I
MATERIAL PRE-IRRADIATION

Sample	Defect	Level (meV)	Cross Section (cm ²)		Concentration (cm ⁻³)
			Direct Measurement	From Intercept	
Ge 77-85-4	114 (est.)	E _V + 200	-	-	~8 × 10 ¹⁰
Phosphorus doped (1)	116	E _C - 150	-	8.9 × 10 ⁻¹⁵	1.3 × 10 ¹¹
n-type n=8 × 10 ¹³ cm ⁻³ (77 K)	169	E _V + 360	-	3.2 × 10 ⁻¹⁵	1.4 × 10 ¹¹
Ge 77-93-4					
Arsenic doped (1)	no individual peaks				3 × 10 ¹⁰ minority ~10 ¹⁰ majority
n-type n=2.2 × 10 ¹⁴ cm ⁻³ (77 K)					
Ge 78-93-4	20 (est.)	E _C - 42	-	-	
Undoped (1)	30	E _C - 62	-	-	1.4 × 10 ⁹
p-type	37	E _C - 65	-	-	
p=4.3 × 10 ¹⁰ cm ⁻³ (77 K)	40	E _V + 68	4.6 × 10 ⁻¹⁴	7.9 × 10 ⁻¹⁴	8.1 × 10 ⁸
Ge 78-93-6	118	E _C - 220	-	-	5.3 × 10 ⁹
Undoped (1)	163	E _C - 270	-	-	5.8 × 10 ⁹
n-type n=3.3 × 10 ¹² cm ⁻³ (77 K)					
Ge 78-8-6-1	no individual peaks				~5 × 10 ⁹ for electron and hole traps
Undoped (2)					
p-type p=2.7 × 10 ¹² cm ⁻³ (77 K)					
Ge 78-8-6	87	E _V + 180	-	6.6 × 10 ⁻¹³	1.1 × 10 ¹⁰
Undoped (2) (3)	104	E _V + 210	7.7 × 10 ⁻¹⁴	1.7 × 10 ⁻¹³	3.7 × 10 ¹⁰
p-type (hydrogen free)	142	E _V + 330	6.3 × 10 ⁻¹³	3.2 × 10 ⁻¹²	5.6 × 10 ¹⁰
p=9.6 × 10 ¹² (77 K)					

TABLE 1 (Continued)

Sample	Defect	Level (meV)	Cross Section (cm ³)		Concentration (cm ⁻³)
			Direct Measurement	From Intercept	
Ge 78-48-9 Undoped (4) Wet N ₂ n-type n=3.2 × 10 ¹³ cm ⁻³ (77 K)	no individual peaks				~ 5 × 10 ⁹ majority ~ 7 × 10 ¹¹ minority
Ge 78-48-4 Undoped (5) dry N ₂ n-type n=1.1 × 10 ¹¹ cm ⁻³ (77 K)	no individual peaks				~ 2 × 10 ⁹ minority ~ 10 ⁷ majority

NOTE:

- (1) Crystal pulled from high-purity 'Spectrosil' silica crucible under hydrogen (palladium-diffused).
- (2) Crystal pulled from high-purity 'UF45' graphite crucible under hydrogen (palladium-diffused).
- (3) Sample was made hydrogen deficient by heating under high-purity nitrogen at 650°C for 74 hours.
- (4) Crystal pulled under wet, high-purity nitrogen (gas bubbled through water at approx. 20°C).
- (5) Crystal pulled under dry, high-purity nitrogen.

TABLE 2
MATERIAL POST-IRRADIATION (1500 kGy (150 Mrad), ^{60}Co gammas)

Sample	Defect	Level (meV)	Cross Section (cm^2)		Concentration (cm^{-3})
			Direct Measurement	From Intercept	
Ge 77-85-4	13	$E_V + 18$	-	-	6.7×10^9
Phosphorus doped	113 (est.)	$E_V + 200$	-	-	$\sim 10^9$
n-type	135 (est.)	$E_V + 280$	-	-	9.3×10^9
$n=1.3 \times 10^{10} \text{ cm}^{-3}$ (13 K)	163	$E_C - 0.45$	1.3×10^{-14}	1.4×10^{-14}	2.5×10^{11}
$=2.4 \times 10^{10} \text{ cm}^{-3}$ (77 K)					
$=7.3 \times 10^{10} \text{ cm}^{-3}$ (130 K)					
$=3.2 \times 10^{12} \text{ cm}^{-3}$ (165 K)					
Ge 77-93-4	88	$E_C - 180$	2.5×10^{-15}	5.6×10^{-15}	1.4×10^{11}
Arsenic doped	103	$E_C - 190$	4.9×10^{-16}	6.9×10^{-17}	1.6×10^{11}
n-type	163	$E_C - 0.40$	3.7×10^{-14}	1.0×10^{-14}	1.6×10^{11}
$n=5.9 \times 10^{12} \text{ cm}^{-3}$ (77 K)					
$6.2 \times 10^{12} \text{ cm}^{-3}$ (103 K)					
$7.3 \times 10^{12} \text{ cm}^{-3}$ (163 K)					
Ge 78-93-4	31	$E_V + 35$	$\sim 10^{-17}$	1.0×10^{-18}	1.8×10^{11}
Undoped	38	$E_V + 43$	-	7.8×10^{-16}	2.9×10^{10}
p-type	55	$E_V + 87$	$\sim 10^{-17}$	4.7×10^{-16}	5.6×10^{10}
$p=2.9 \times 10^{12} \text{ cm}^{-3}$ (31 K)	64	$E_V + 104$	-	5.7×10^{-15}	1.3×10^{10}
$3.2 \times 10^{12} \text{ cm}^{-3}$ (55 K)	105	$E_V + 260$	7.5×10^{-15}	3.0×10^{-13}	3.2×10^{12}
$4.0 \times 10^{12} \text{ cm}^{-3}$ (77 K)	163	$E_V + 400$	1.3×10^{-14}	1.3×10^{-13}	1.3×10^{12}
$5.3 \times 10^{12} \text{ cm}^{-3}$ (105 K)					
$1.1 \times 10^{13} \text{ cm}^{-3}$ (163 K)					
Ge 78-93-6	24	$E_V + 21$	-	$\sim 5 \times 10^{-18}$	5.7×10^{10}
Undoped	25 (75 ms)	$E_V + 30$ (est.)	-	-	$\sim 5.7 \times 10^{10}$
n-type	45	$E_V + 45$	-	4.3×10^{-15}	8.4×10^{10}
$n=6.2 \times 10^{10} \text{ cm}^{-3}$ (24 K)	97 (est.)	$E_V + 130$	-	-	3.1×10^{11}
$1.7 \times 10^{11} \text{ cm}^{-3}$ (77 K)	Continuum of levels from 65 K - 110 K, i.e. from $E_V + 100$ to 150 meV				

TABLE 2 (Continued)

Sample	Defect	Level (meV)	Cross Section (cm ²)		Concentration (cm ⁻³)
			Direct Measurement	From Intercept	
Ge 78-8-6	28	E _v + 32	1.9 × 10 ⁻¹⁶	5.9 × 10 ⁻¹⁸	7.2 × 10 ¹¹
Undoped	41	E _v + 69	-	2.2 × 10 ⁻¹⁶	3.2 × 10 ¹⁰
p-type	53	E _v + 92	-	2.8 × 10 ⁻¹⁶	8.0 × 10 ¹⁰
p=1.6 × 10 ¹³ cm ⁻³ (28 K)	67	E _v + 100	-	1.8 × 10 ⁻¹⁴	5.6 × 10 ¹⁰
2.4 × 10 ¹³ cm ⁻³ (77 K)	110	E _v + 230	6.7 × 10 ⁻¹⁵	1.7 × 10 ⁻¹⁴	2.9 × 10 ¹²
2.8 × 10 ¹³ c (110 K)	163	E _v + 380	9.0 × 10 ⁻¹⁵	3.1 × 10 ⁻¹⁴	1.3 × 10 ¹²
3.3 × 10 ¹³ cm ⁻³ (163 K)					
Ge 78-8-6	84	E _v + 160	-	1.1 × 10 ⁻¹⁵	9.0 × 10 ¹⁰
Undoped	103	E _v + 200	3.0 × 10 ⁻¹⁵	1.3 × 10 ⁻¹⁵	1.1 × 10 ¹¹
p-type	135 (est.)	E _v + 290	-	-	6 × 10 ¹⁰
p=3.7 × 10 ¹³ cm ⁻³ (77 K)	145 (est.)	E _v + 320	-	-	6 × 10 ¹⁰
3.9 × 10 ¹³ cm ⁻³ (103 K)	169	E _v + 380	4.2 × 10 ⁻¹⁴	1.5 × 10 ⁻¹⁴	1.6 × 10 ¹¹
4.3 × 10 ¹³ cm ⁻³ (169 K)					
Ge 78-48-9	152	E _c - 270	5.8 × 10 ⁻¹⁶	1.0 × 10 ⁻¹⁷	2.3 × 10 ¹²
Wet N ₂	185 (est.)	E _c - 420	-	-	2.2 × 10 ¹¹
Undoped					
n-type					
n=4.4 × 10 ¹² cm ⁻³ (77 K)					
9.1 × 10 ¹² cm ⁻³ (152 K)					
Ge 78-48-4	81	E _v + 120	-	-	8.2 × 10 ⁸
Undoped	110	E _v + 240	-	3.2 × 10 ⁻¹⁶	1.7 × 10 ¹⁰
n-type	165	E _c - 420	6.4 × 10 ⁻¹⁴	1.3 × 10 ⁻¹³	2.1 × 10 ¹²
n=2.6 × 10 ¹⁰ cm ⁻³ (77 K)					
3.2 × 10 ¹⁰ cm ⁻³ (110 K)					
1.2 × 10 ¹³ cm ⁻³ (165 K)					

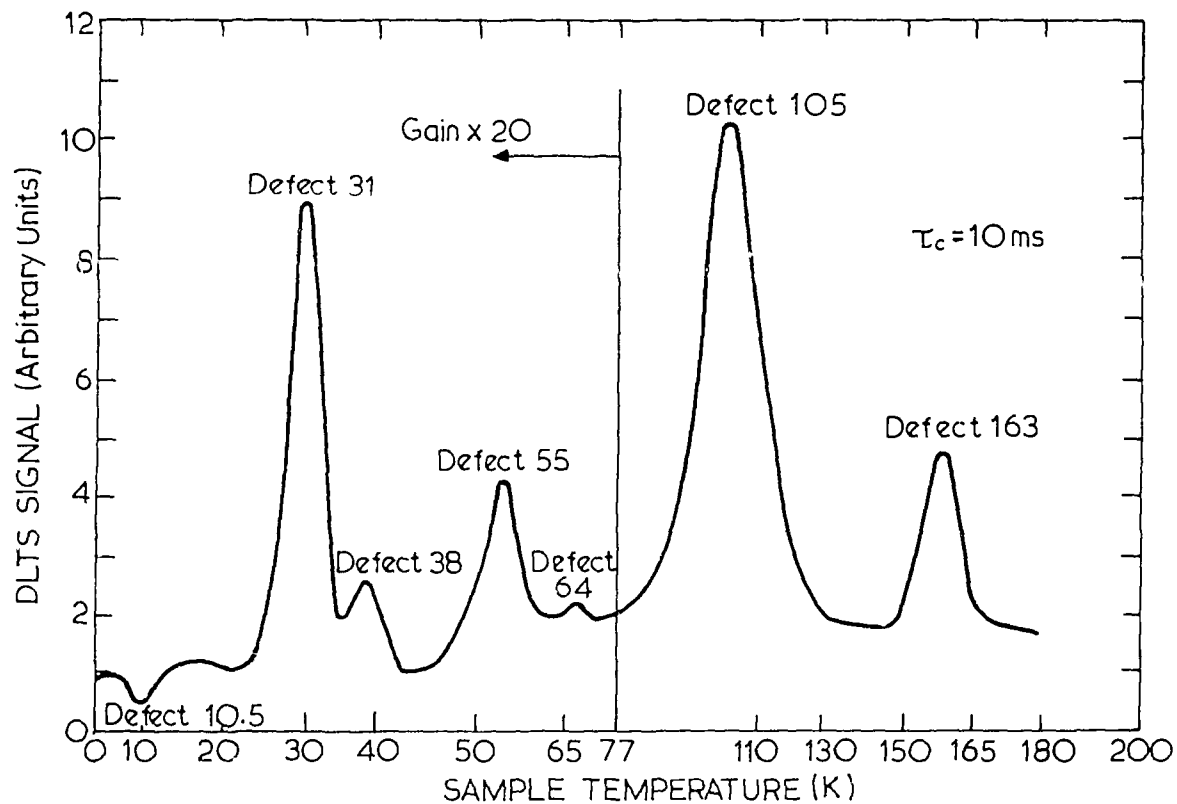


FIGURE 1. DLT SPECTRUM OF 78-93-4 POST-IRRADIATION
(CORRELATOR TIME CONSTANT $\tau_c = 10\text{ ms}$)

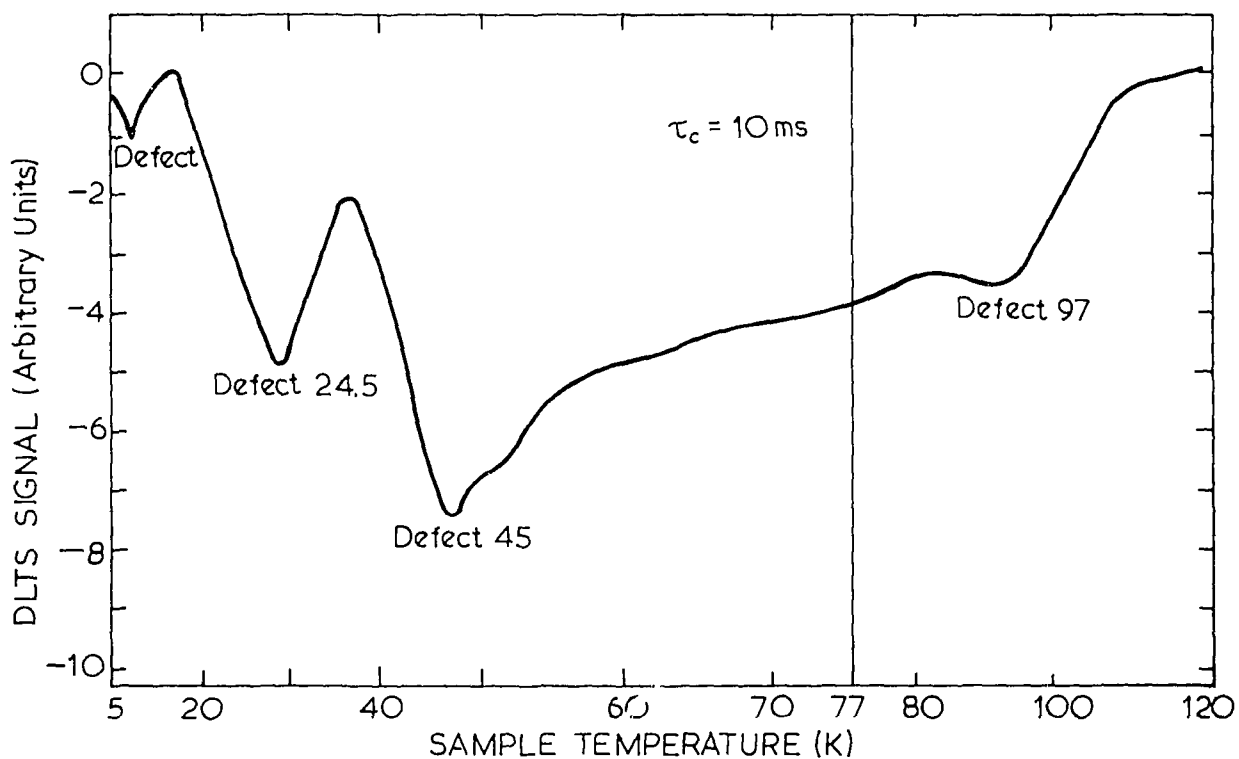


FIGURE 2. DLT SPECTRUM OF 78-93-6 POST-IRRADIATION

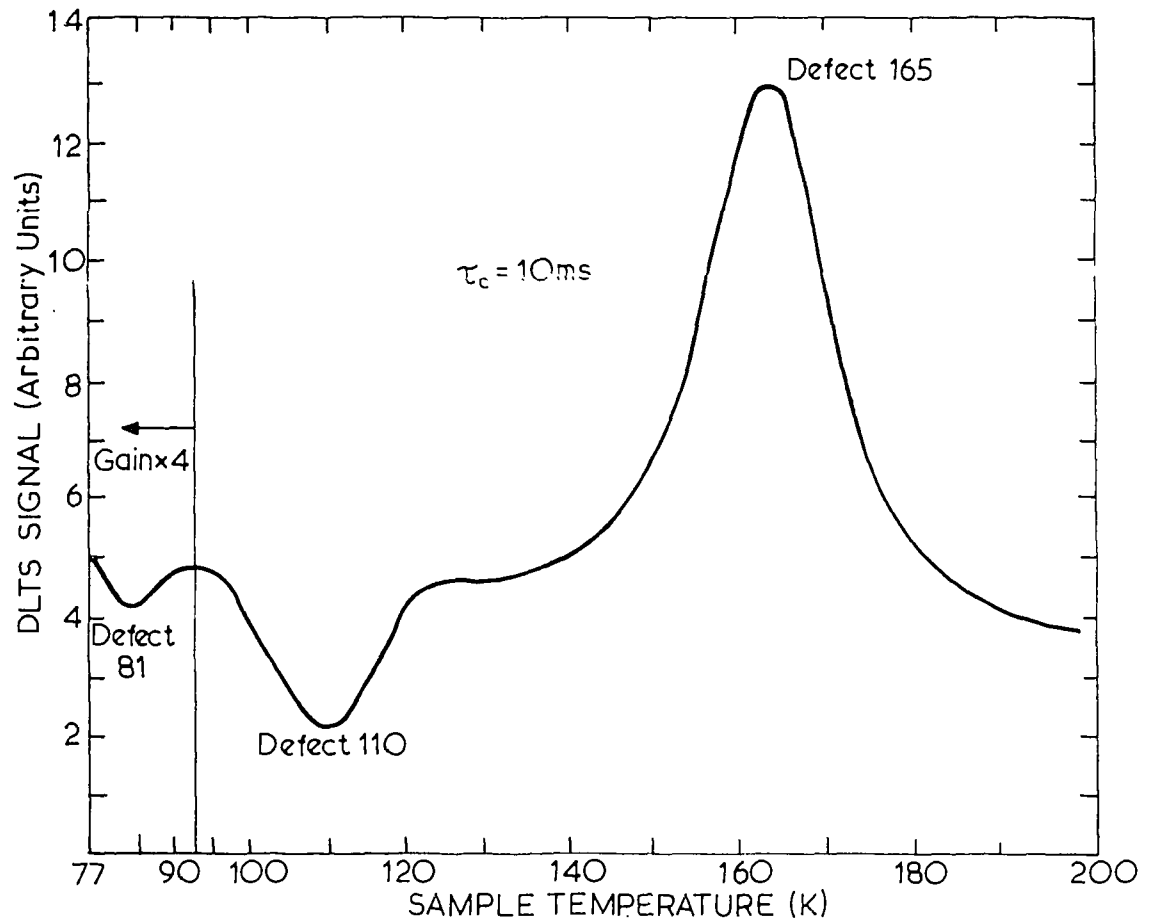


FIGURE 3. DLT SPECTRUM OF 78-48-4 POST-IRRADIATION

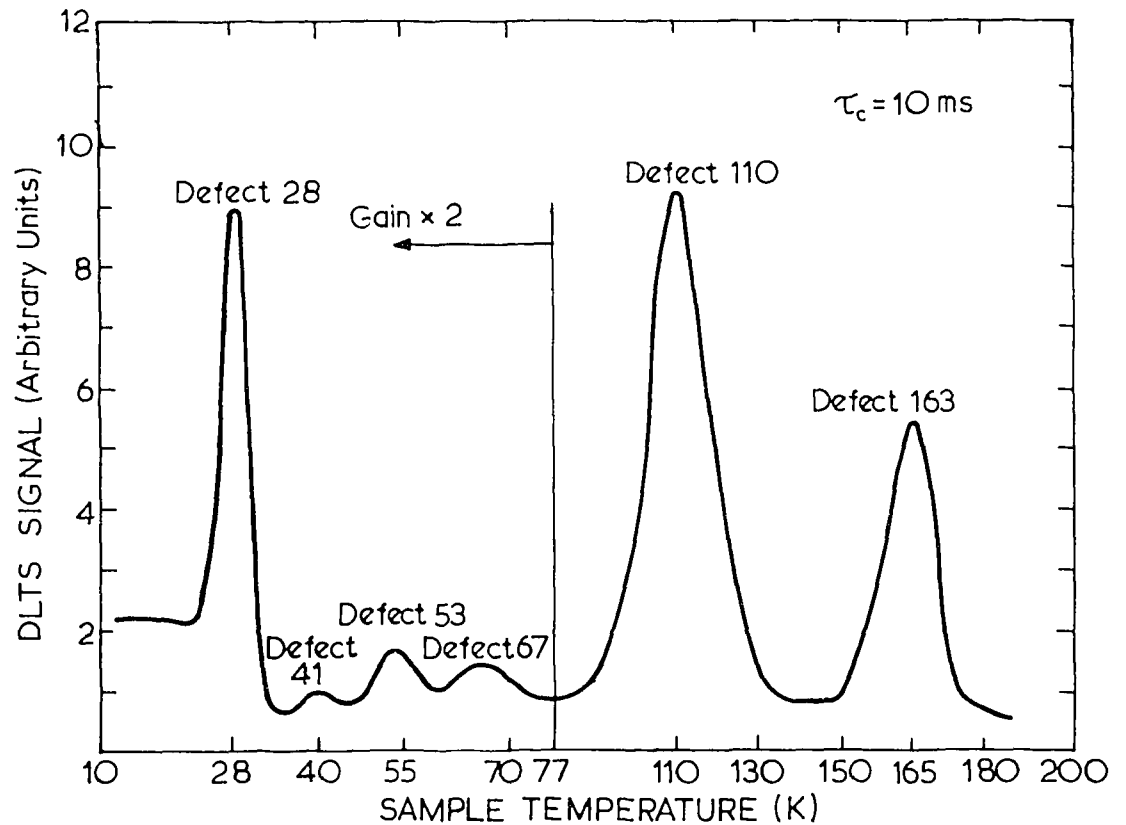


FIGURE 4. DLT SPECTRUM OF 78-8-6 (H₂-RICH) POST-IRRADIATION

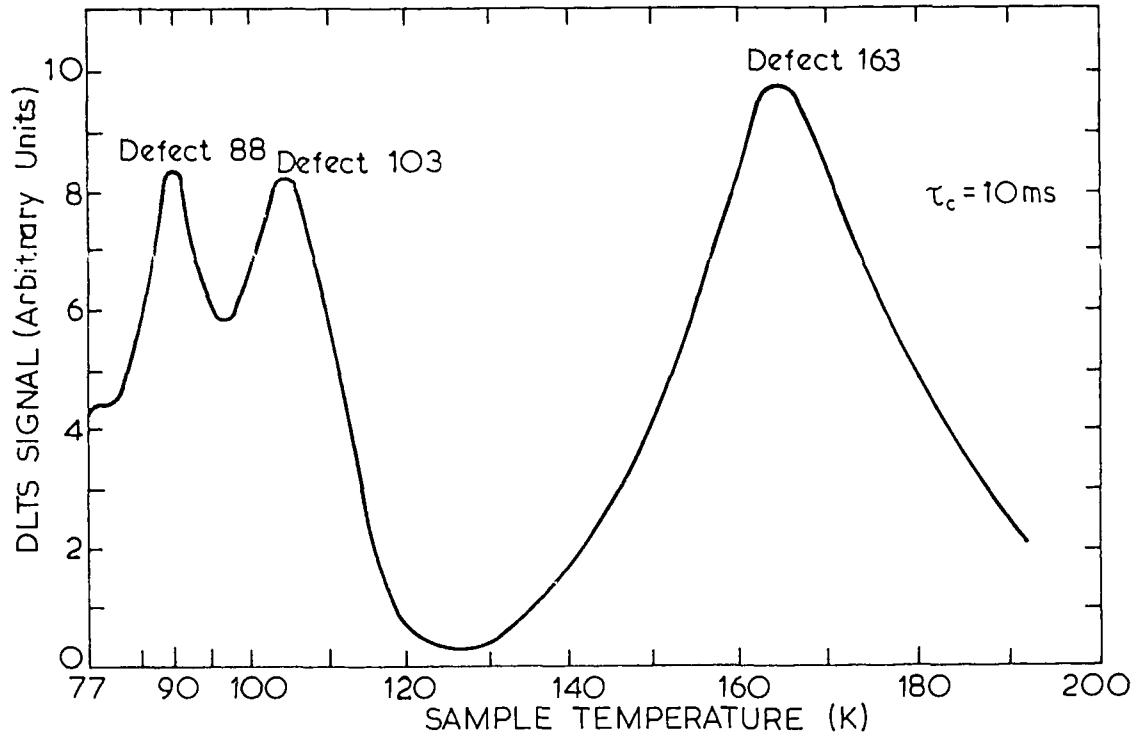


FIGURE 5. DLT SPECTRUM OF 77-93-4 POST-IRRADIATION

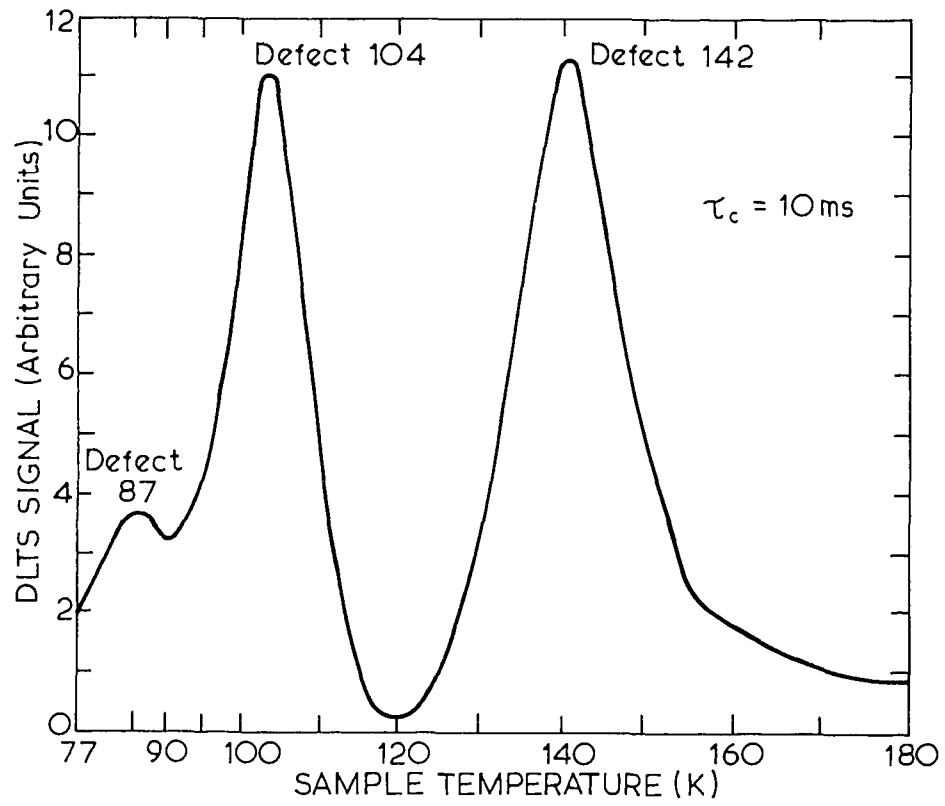


FIGURE 6. DLT SPECTRUM OF 78-8-6 (H₂-POOR) PRE-IRRADIATION

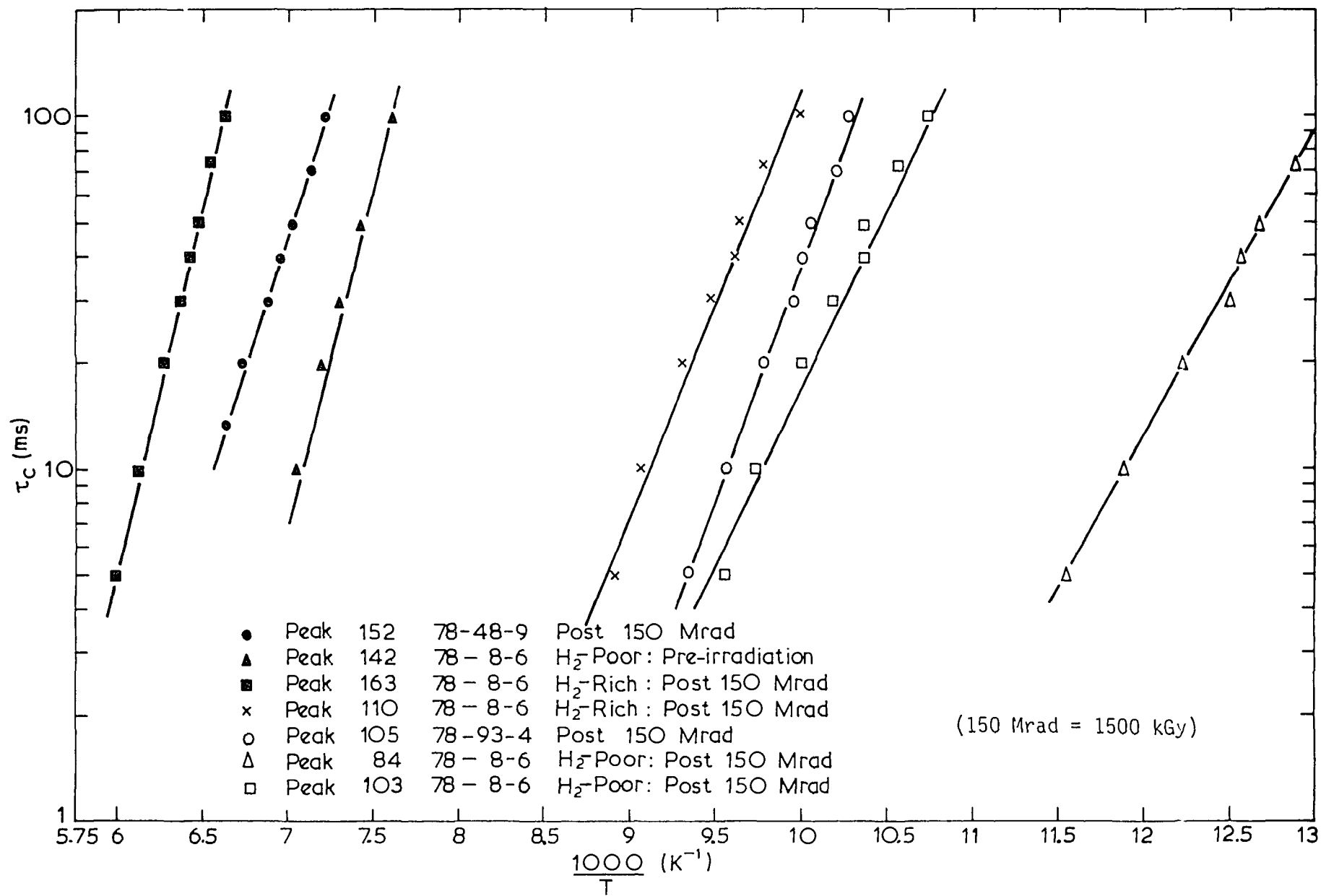


FIGURE 7. ARRHENIUS PLOTS FOR SOME DEFECT LEVELS OBSERVED IN GERMANIUM

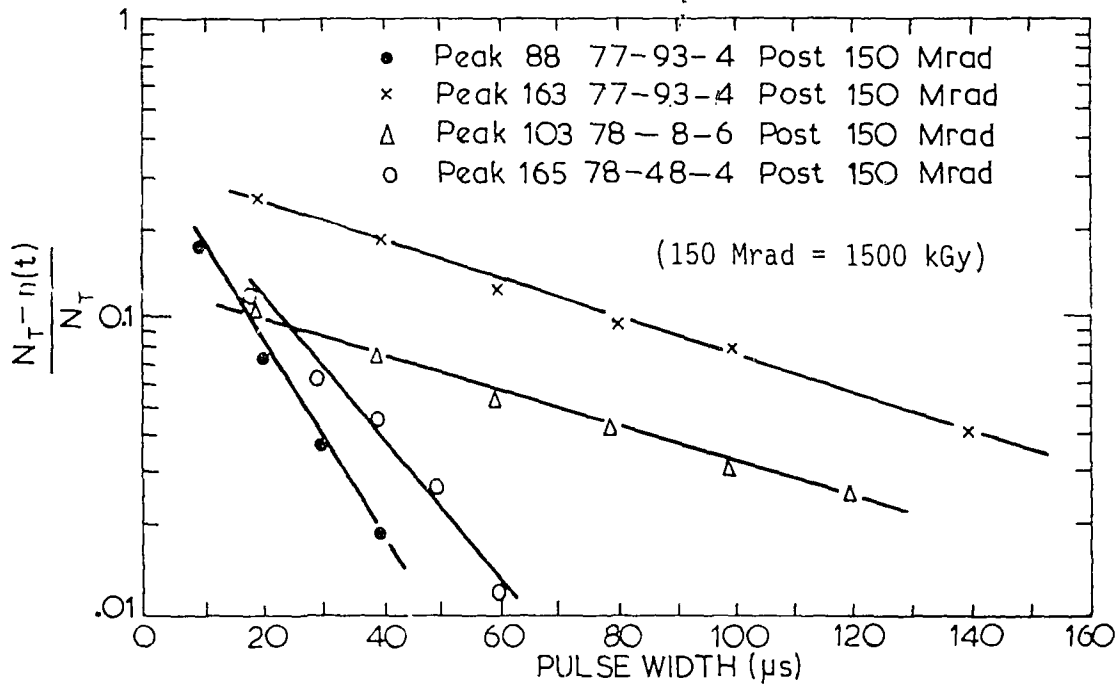


FIGURE 8. RELATIVE SIGNAL OUTPUT v. PULSE WIDTH FOR SOME DEFECT LEVELS IN GERMANIUM

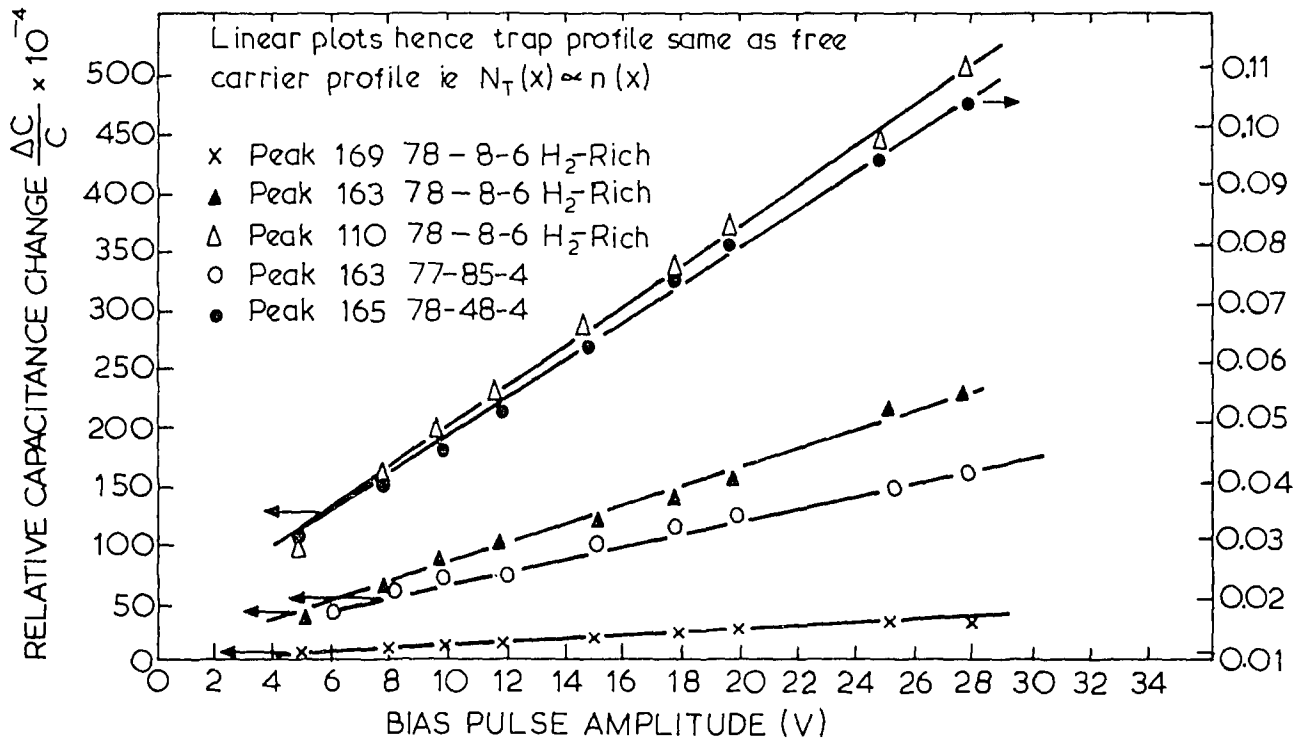


FIGURE 9. RELATIVE CAPACITANCE CHANGE v. PULSE AMPLITUDE FOR SOME DEFECT LEVELS IN GERMANIUM

